Inverse-Compton drag on a highly magnetized GRB jet in stellar envelope

Ceccobello, C.; Kumar, P.

Link to publication

Inverse-Compton drag on a highly magnetized GRB jet in stellar envelope

Chiara Ceccobello[1,2]⋆ and Pawan Kumar[3]⋆

[1] *'Anton Pannekoek' Instituut voor Sterrenkunde, Universiteit van Amsterdam, Science Park 904, NL-1098 XH Amsterdam, the Netherlands*
[2] *Dipartimento di Fisica, Università di Ferrara, via Saragat 1, I-44122 Ferrara, Italy*
[3] *Department of Astronomy, University of Texas at Austin, TX 78712, USA*

ABSTRACT

The collimation and evolution of relativistic outflows in γ-ray bursts are determined by their interaction with the stellar envelope through which they travel before reaching the much larger distance where the energy is dissipated and γ-rays are produced. We consider the case of a Poynting-flux-dominated relativistic outflow and show that it suffers strong inverse-Compton (IC) scattering drag near the stellar surface and the jet is slowed down to sub-relativistic speed if its initial magnetization parameter (σ_0) is larger than about 10^5. If the temperature of the cocoon surrounding the jet were to be larger than about 10 keV, then an optically thick layer of electrons and positrons forms at the interface of the cocoon and the jet, and one might expect this pair screen to protect the interior of the jet from IC drag. However, the pair screen turns out to be ephemeral, and instead of shielding the jet it speeds up the IC drag on it. Although a high σ_0 jet might not survive its passage through the star, a fraction of its energy is converted to 1–100 MeV radiation that escapes the star and appears as a bright flash lasting for about 10 s.

Key words: scattering – gamma-ray burst: general – stars: jets – stars: magnetic field.

1 INTRODUCTION

Long gamma-ray bursts (long GRBs) are explosions resulting from the core collapse of massive stars at the end of their nuclear burning life cycle. The amount of energy produced in these explosions is estimated to be $\sim 10^{48}$–10^{52} erg (e.g. Sari, Piran & Halpern 1999; Frail et al. 2001; Panaitescu & Kumar 2001; Berger, Kulkarni & Frail 2003; Curran, van der Horst & Wijers 2008; Liang et al. 2008; Racusin et al. 2009; Cenko et al. 2010). The collapse of the core of a GRB progenitor produces either a black hole or a neutron star, and in either case the central compact object is believed to be rapidly rotating (for a review, Piran 1999; Meszaros 2006; Woosley & Bloom 2006; Gehrels, Ramirez-Ruiz & Fox 2009). As in other astrophysical sources such as active galactic nuclei (AGN), microquasars, pulsars and SGRs (soft-gamma-ray repeaters), a rapidly rotating black hole, or a magnetar, is expected to produce a relativistic bipolar jet which then interact with the ambient medium (e.g. Falcke, Körding & Markoff 2004; Markoff, Nowak & Wilms 2005; Bucciantini et al. 2008, 2009; Narayan & McClintock 2008; Markoff 2010; Yuan & Narayan 2014).

In the scenario where the central engine of a GRB is a rapidly rotating magnetar, a Poynting-flux-dominated jet is generated by the

strong magnetic field with an initial jet magnetization parameter,[1] σ_0, of the order of $\sim 10^3$ (Thompson, Chang & Quataert 2004; Metzger, Thompson & Quataert 2007). The magnetization parameter increases as the neutrino-driven baryonic mass-loss rate at the surface of the neutron star decreases on de-leptonization time-scale of about half a minute (Metzger et al. 2011). In fact, the increase to the magnetization parameter can be rather dramatic with $\sigma_0 \sim 10^9$ as the neutrino luminosity winds down (Metzger et al. 2011). These authors associate the transition to high σ_0 with the end of the prompt gamma-ray phase and the steep decline of X-ray afterglow that is seen for a large fraction of bursts detected by the *Swift* satellite (Tagliaferri et al. 2005; O'Brien et al. 2006; Willingale et al. 2010). The reason for this association, according to Metzger et al. (2011), is that the acceleration and dissipation are very inefficient processes for high σ_0 jets. It should be noted that highly magnetized jets are not limited to the magnetar model, but could also be produced when the GRB central engine is an accreting black hole as the mechanism for launching of the jet might be the Blandford–Znajek process (Blandford & Znajek 1977). In this paper, we address the question regarding the survival of a highly magnetized jet ($\sigma_0 \gtrsim 10^4$) as it propagates through the GRB progenitor star and is exposed an

---

⋆ E-mail: c.ceccobello@uva.nl (CC); pk@surya.as.utexas.edu (PK)

[1] Magnetization parameter is defined as the ratio of Poynting flux and particle kinetic energy flux carried by the jet.

intense radiation field that can penetrate all the way to jet axis and can drag it down.

Inverse-Compton (IC) drag has been considered by a number of people for AGN jets e.g. Phinney (1987), Melia & Konigl (1989), Sikora et al. (1996), Ghisellini, Tavecchio & Chiaberge (2005), Ghisellini & Tavecchio (2010). However, the GRB jets are different in that they are highly opaque throughout much of the region where they undergo acceleration (as opposed to AGN jets which are transparent throughout their entire length), and thus the IC drag on GRB jets due to an external field can be treated independently of the acceleration mechanism.

A jet propagating through the GRB progenitor star envelope creates a hot cocoon within which the jet is enclosed by the time it reaches the stellar surface. We describe the interaction of such highly magnetized jets with photons from the hot cocoon and how that affects the jet propagation through the envelope of the progenitor star. In particular, we analyse the role of the IC drag in braking the relativistic outflow.

The organization of this paper is as follows. In the next section, we calculate how far inside the jet can X-ray photons from the cocoon penetrate the jet, and at the distance from the centre when the jet becomes transparent. Section 3 provides an estimate for IC drag on a high magnetization parameter jet due to scattering of X-ray photons from the cocoon surrounding it, but ignoring the creation of $e^{\pm}$ pairs and possible shielding of the jet provided by these particles. In Section 4, we consider whether the core of the jet could be shielded by electron–positron pairs produced either at the base of the jet or at the interface of the jet and cocoon by collision of X-ray photons with gamma-ray photons that are arise when X-ray photons are IC scattered by electrons in the jet.

2 PHOTOSPHERIC RADIUS FOR POYNTING-FLUX-DOMINATED JETS

Let us consider a relativistic Poynting-dominated jet composed by a mixture of baryons, leptons and photons. As seen in the frame comoving with the flow, baryons and leptons are thermally distributed and have the same number density.

The total isotropic equivalent luminosity of a Poynting jet, which has significant thermal energy, and where mass flux is dominated by baryons, can be written as

$$L = \pi R^2 \theta_j^2(R) \left[m_p n_p' v c^2 \Gamma^2 + \frac{4}{3} u_\gamma' \Gamma^2 v + \frac{B'^2 \Gamma^2 v}{4\pi} \right], \qquad (1)$$

where Γ and v are jet Lorentz factor and speed, n_p' and B' are jet comoving frame proton density and magnetic field strength, u_γ' is the energy density in photons in jet comoving frame, and $\theta_j(R)$ is the jet half-opening angle when it is at radius R.

Using the mass conservation equation and the definition of the magnetization parameter, which are the following:

$$\dot{M}_\pm = \pi \theta_j^2 R^2 m_p n_p' \Gamma v \qquad (2)$$

$$\sigma = \frac{B'^2}{4\pi m_p n_p' c^2}, \qquad (3)$$

we obtain

$$L = \dot{M}_\pm c^2 \Gamma \left(1 + \xi + \sigma \right), \qquad (4)$$

where

$$\xi \equiv \frac{4 u_\gamma'}{3 m_p n_p' c^2} \qquad (5)$$

is the ratio of thermal energy and baryon rest-mass energy densities. From equations (2)–(4), we calculate proton number density in the comoving frame

$$n_p'(R) \approx \frac{L}{\Gamma_0(1 + \xi_0 + \sigma_0)c^2} \frac{1}{\pi \theta_j^2 R^2 m_p c \Gamma}$$

$$\approx \frac{L}{\pi \theta_j^2 R^2 m_p c^3 (\sigma_0 + \xi_0) \Gamma}, \qquad (6)$$

where Γ_0, ξ_0 and σ_0 are values at the base of the jet at radius R_0, and the last part of the above equation is obtained by assuming that $\Gamma_0 \sim 1$ and $\sigma_0 + \xi_0 \gg 1$.

While the jet is inside the star, it is collimated by the pressure of the cocoon and the ambient stellar medium, and we take its Lorentz factor to increase with radius as

$$\Gamma \sim \left[\frac{r}{R_0} \right]^\alpha, \qquad (7)$$

as long as $\Gamma < (\xi_0 + \sigma_0)$. The index α in the above equation can be shown to be related to the pressure (p) stratification of GRB progenitor star; for $p \propto r^{-a}$, $\alpha = a/4$ as long as $a \le 2$ (Kumar & Zhang 2014). The pressure in the He-envelope of the GRB progenitor star declines as $\sim r^{-2}$, and therefore we expect $\alpha \sim 0.5$ for a Poynting jet. The transverse size of the jet increases with radius in the same way as Γ (Kumar & Zhang 2014), i.e.

$$R_{j,\perp}(r) \sim R_0 \left[\frac{r}{R_0} \right]^\alpha, \qquad (8)$$

and therefore the jet angle is given by

$$\theta(r) \sim \left[\frac{R_0}{r} \right]^{1-\alpha}. \qquad (9)$$

The photospheric radius where the Thompson optical depth of the jet in the jet-longitudinal direction is unity, is determined from

$$\tau_T \approx \int \frac{dr}{2\Gamma^2} \sigma_T n_p'(r) \Gamma \approx \frac{\sigma_T L}{2\pi(4\alpha - 1)R_0 m_p c^3 (\sigma_0 + \xi_0)} \left[\frac{R_0}{R} \right]^{4\alpha - 1}, \qquad (10)$$

where we made use of equation (6) for electron number density (which is assumed to be equal to proton number density), and equations (7) and (9) to substitute for Γ and θ_j, respectively. Thus the photospheric radius is

$$R_{ph} = R_0 \left[\frac{\sigma_T L}{2\pi(4\alpha - 1)m_p c^3 (\sigma_0 + \xi_0)R_0} \right]^{\frac{1}{4\alpha - 1}}$$

$$\sim \left(2.4 \times 10^9 \text{cm} \right) L_{50} \sigma_{0,6}^{-1} \left(\Gamma_2 \theta_{j,-1} \right)^{-2}. \qquad (11)$$

So in case of initially large magnetization parameter ($\gtrsim 10^4$), photons can escape from the jet well before the jet reaches the stellar surface. We note that the maximum Lorentz factor of a thermal fireball with $\sigma_0 = 0$ is obtained when the jet acceleration continues out to the photospheric radius R_{ph} and is given by $\Gamma_{max} \sim [\sigma_T L/(2\pi(4\alpha - 1)m_p c^3 R_0)]^{\alpha/(5\alpha-1)}$ as long as $R_{ph} < R_*$; for $\alpha = 1$, $\Gamma_{max} \sim 5.4 \times 10^2 L_{51}^{1/4} R_{0,7}^{-1/4}$.

Photons from the cocoon surrounding the jet cannot penetrate very far inside the jet at radius R_{ph} because of the much larger optical depth in the transverse direction. To estimate the IC drag of the jet due to scattering of X-ray photons from the cocoon by electrons in the jet, we first determine the radius where the jet becomes transparent in the transverse direction.
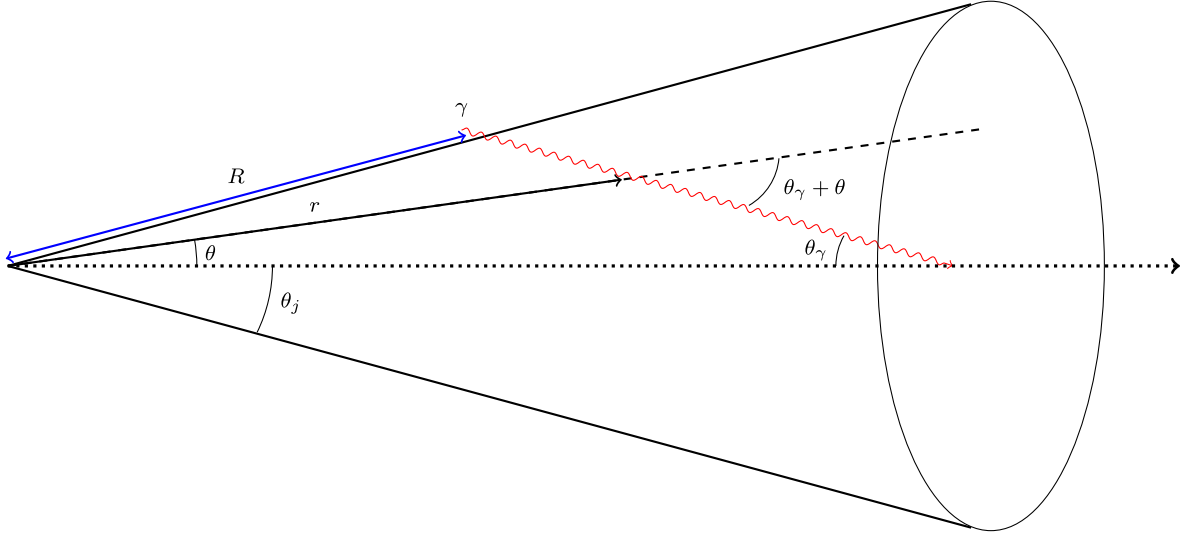
Figure 1. Schematic sketch of a photon trajectory (red line) from the hot cocoon passing through the jet axis (dotted line). The angle between the photon initial direction of motion and the jet axis is labelled as θ_γ and the jet opening angle is θ_j. R is the radial distance between the centre of explosion and the injection point where the cocoon photon enters the jet and r is the radial coordinate. Although the jet is shown to be conical in this representation, its transverse radius increases more slowly than r while it is confined by the pressure of the star/cocoon.

2.1 Jet transparency radius in the transverse direction

The optical depth of the jet for photons of frequency ν_c travelling in a direction perpendicular to the jet axis, including Klein–Nishina correction to the scattering cross-section, is

$$
\begin{aligned}
\tau_\perp(r) &\approx \frac{\sigma_T n_p'(r)\Gamma\theta_j r}{1+h\nu_c\Gamma/(m_e c^2)}\left[1+2\ln\left(1+\frac{2h\nu_c\Gamma}{m_e c^2}\right)\right] \\
&\approx \frac{\sigma_T L}{\pi\theta_j m_p c^3(\sigma_0+\xi_0)r[1+h\nu_c\Gamma/(m_e c^2)]},
\end{aligned}
\tag{12}
$$

where we used equation (6) for n_p'. The radius where the jet becomes transparent to photons moving in the transverse direction is

$$
R_{\mathrm{ph},\perp} \approx \left(5\times10^{12}\mathrm{cm}\right)\frac{L_{50}\sigma_{0,6}^{-1}}{\theta_{j,-1}[1+h\nu_c\Gamma/(m_e c^2)]}.
\tag{13}
$$

A more general situation is where photons are travelling at an angle θ_γ with respect to the jet axis. We calculate the optical depth for these photons to travel from the interface of jet and the cocoon to the jet axis. Consider a photon travelling at an angle θ_γ with respect to jet axis and electrons moving in the radial direction (see Fig. 1). The optical depth for a photon of frequency to scatter off electrons along its trajectory starting from cocoon–jet interface to the jet axis is

$$
\tau(\theta_\gamma) \approx \int_0^{\theta_j} \mathrm{d}\theta\, r\, \frac{\sigma_T n_p(r)[1-v\cos(\theta+\theta_\gamma)/c]}{[1+h\nu'/m_e c^2]\sin(\theta+\theta_\gamma)},
\tag{14}
$$

where $n_p = \Gamma n_p'$ is electron density in star rest frame,

$$
\nu_c'(\theta+\theta_\gamma) = \nu_c\Gamma\left[1-v\cos(\theta+\theta_\gamma)/c\right],
\tag{15}
$$

is photon frequency in electron rest frame, and we have assumed that there is one electron per proton in the jet; Klein–Nishina correction to Thompson cross-section is included in equation (14). The photon trajectory in the polar coordinate is described by (see Fig. 1)

$$
r\sin(\theta+\theta_\gamma) = R\sin(\theta_j+\theta_\gamma).
\tag{16}
$$

Using

$$
n_p(r) = \frac{L}{\pi\theta_j^2 r^2 m_p c^3(\sigma_0+\xi_0)} = (7\times10^{17}\mathrm{cm}^{-3})\frac{L_{50}}{\theta_{j,-1}^2 r_{10}^2(\sigma_{0,6}+\xi_{0,6})},
\tag{17}
$$

we find

$$
\tau = \frac{\sigma_T L}{\pi\theta_j^2 m_p c^3(\sigma_0+\xi_0)}\int_0^{\theta_j}\mathrm{d}\theta\,\frac{[1-v\cos(\theta+\theta_\gamma)/c]}{r[1+h\nu_c'(\theta+\theta_\gamma)/m_e c^2]\sin(\theta+\theta_\gamma)}.
\tag{18}
$$

With use of equation (16) for r, this reduces to

$$
\begin{aligned}
\tau(r) &\approx \frac{\sigma_T L\left[1+h\nu_c'(\theta_\gamma)/m_e c^2\right]^{-1}}{\pi\theta_j^2 m_p c^3(\sigma_0+\xi_0)r\sin(\theta_j+\theta_\gamma)} \\
&\times\left[\theta_j - v\left\{\sin(\theta_j+\theta_\gamma)-\sin\theta_\gamma\right\}/c\right].
\end{aligned}
\tag{19}
$$

The GRB jet Lorentz factor near the surface of the progenitor star is expected to be much larger than θ_j^{-1}. In that case for $\theta_\gamma \ll \theta_j$, equation (19) reduces to

$$
\tau \approx 1.5L_{50}(\sigma_{0,6}+\xi_{0,6})^{-1}r_{11}^{-1}\left[1+h\nu_c'(\theta_\gamma)/m_e c^2\right]^{-1},
\tag{20}
$$

and for $\theta_\gamma \gg \theta_j$ the expression for optical depth reduces to equation (12). The jet optical depth in the transverse direction at a given radius for these two limiting cases differs by a factor ~10.

3 IC DRAG FOR POYNTING-FLUX-DOMINATED JETS

We calculate the IC loss for an electron when it is exposed to a beam of photons moving at an angle θ_γ with respect to electron velocity. The electron moves with the jet and therefore its Lorentz factor and velocity are Γ and v, respectively. Let us consider the specific intensity of the photon beam from the cocoon in the rest frame of the star to be $I_\nu(\theta_\gamma)$. The transformations of photon frequency, specific intensity and angle from star rest frame to jet comoving frame are

given by

$$\nu' = \nu\Gamma(1 - v\cos\theta_\gamma/c), \qquad I'_{\nu'}(\theta') = I_\nu(\nu'/\nu)^3,$$
$$\sin\theta' = (\nu/\nu')\sin\theta_\gamma. \tag{21}$$

The rate of loss of energy for an electron due to IC scatterings is proportional to photon energy flux in its comoving frame. Using the above transformations, the comoving flux can be shown to be proportional to $\theta_\gamma^2\Gamma^2(1 - v\cos\theta_\gamma/c)^2 \propto \theta_\gamma^6\Gamma^2$ for $\Gamma\theta_\gamma > 1$. Thus, the IC drag on electrons increases very rapidly with increasing θ_γ, and that nearly compensates for the smaller flux at the jet axis due to larger optical depth for larger θ_γ. So from here on we specialize to $\theta_\gamma \sim 1$. Consider a photon of frequency ν_c scattered by an electron of Lorentz factor Γ. In the comoving frame, the scattered photon energy is

$$h\nu'_{ic} = \frac{h\nu'_c}{1 + \frac{h\nu'_c}{m_e c^2}(1 - \cos\theta_\gamma)}. \tag{22}$$

The average energy of the scattered photon in the Klein–Nishina limit can be calculated as

$$\langle h\nu_{ic}\rangle = \frac{\int d\Omega'_\gamma \frac{d\sigma_{kn}}{d\Omega'_\gamma} h\nu_{ic}}{\int d\Omega'_\gamma \frac{d\sigma_{kn}}{d\Omega'_\gamma}}, \tag{23}$$

where the differential Klein–Nishina cross-section is taken from Blumenthal & Gould (1970). When $2 \lesssim h\nu_c\Gamma/(m_e c^2) \lesssim \Gamma^2$, the average energy of the scattered photon can be shown to be

$$\langle h\nu_{ic}\rangle \approx \frac{2m_e c^2\Gamma}{1 + 2\ln[1 + 2\,h\nu_c\Gamma/(m_e c^2)]}\left[\frac{3m_e c^2}{2\,h\nu_c\Gamma} + \left(1 - \frac{m_e c^2}{h\nu_c\Gamma}\right)\right.$$
$$\left. \times \ln\left(1 + \frac{h\nu_c\Gamma}{2m_e c^2}\right)\right]. \tag{24}$$

The equation for IC drag is

$$\frac{d m_p c^2\Gamma}{dt} \approx -\frac{F_c(t)}{h\nu_c}\sigma_{kn}\,h\nu_{ic}\,\zeta_\pm, \tag{25}$$

where $\zeta_\pm$ is number of electrons and positrons per proton, F_c is cocoon thermal flux given by equation (A23) and the electron–photon scattering cross-section as a function of dimensionless photon energy in electron rest frame ($h\nu_c\Gamma/m_e c^2$) is

$$\sigma_{kn}(h\nu_c\Gamma/m_e c^2) \approx \frac{3\sigma_T}{16\,h\nu_c\Gamma/(m_e c^2)}\left[1 + 2\ln\left(1 + \frac{2h\nu_c\Gamma}{m_e c^2}\right)\right]. \tag{26}$$

In deriving equation (25), we assumed that electrons and protons are coupled and move together.

The IC cooling time in the stellar rest frame for an electron in the jet, at radius r and time t_r after the formation of cocoon, follows from equations (25) and (26):

$$t_{ic}^{kn} \approx \frac{8m_p c^2\Gamma(h\nu_c/m_e c^2)^2}{3\sigma_T\zeta_\pm F_c(t_r)}\left[\frac{3m_e c^2}{2\,h\nu_c\Gamma} + \left(1 - \frac{m_e c^2}{h\nu_c\Gamma}\right)\right.$$
$$\left. \times \ln\left(1 + \frac{h\nu_c\Gamma}{2m_e c^2}\right)\right]^{-1}. \tag{27}$$

Substituting for $h\nu_c = 3k_B T_c$ (equation A16) and F_c (equation A23), we obtain the IC cooling time in Klein–Nishina regime to be

$$t_{ic}^{kn} \sim (8 \times 10^{-5}s)\exp(\tau_\perp)t_r^{1/2}\Gamma_2\eta_{c,1}^{-1/2}\zeta_\pm^{-1}, \tag{28}$$

where η_c is the terminal Lorentz factor of the cocoon. The IC cooling time when the scattering is in the Thompson regime, i.e. $h\nu_c\Gamma \ll m_e c^2$, is given by

$$t_{ic}^{ts} \sim (5 \times 10^{-7}s)\exp(\tau_\perp)t_r^{1/2}\Gamma_2^{-1}\eta_{c,1}^{-1/2}\zeta_\pm^{-1}. \tag{29}$$

The dynamical time at the stellar surface is $R_*/c \sim 3$ s. The IC cooling time is much smaller than this dynamical time as long as the optical depth of the jet in the transverse direction ($\tau_\perp$) is smaller than about 10. equation (27) can be solved to find the radius, R_{CC}, where the IC drag time-scale at the jet-axis (t_{ic}) is comparable to the dynamical time-scale of the jet ($t_{dyn} \sim r/c$), namely

$$\frac{8m_p c^2\Gamma t_r^{1/2}(h\nu_c/m_e c^2)^2}{3\sigma_T\sigma_B T_c^4 t_{fs}^{1/2}e^{-\tau_\perp}\zeta_\pm} \approx \frac{R_{CC}}{c}, \tag{30}$$

where t_r is the time when IC cooling is considered – it is in general larger than the dynamical time since cocoon formation begins with the launch of the relativistic jet and jet duration should exceed R_*/c in order for the jet to break through the stellar surface – and t_{fs} (given by equation A22) in the meantime in between scatterings of a photon while inside the cocoon; the equation is valid for $h\nu_c\Gamma/(m_e c^2) \gg 1$.

Making use of equation (12) for $\tau_\perp$, we can rewrite the above equation for R_{CC} in a more explicit form:

$$\exp\left\{\frac{\sigma_T L}{\pi\theta_j m_p c^3(\sigma_0 + \xi_0)R_{CC}[1 + h\nu_c\Gamma/(m_e c^2)]}\right\}$$
$$= \frac{3\sigma_T\sigma_B T_c^4 t_{fs}^{1/2}\zeta_\pm R_{CC}}{8m_p c^2\Gamma t_r^{1/2}(h\nu_c/m_e c^2)^2}. \tag{31}$$

Equation (31) can be rewritten with the use of equation (7) for Γ

$$e^{A/R_{CC}} = K\,R_{CC}^\beta, \tag{32}$$

where

$$A = \frac{\sigma_T L}{\pi\theta_j m_p c^3(\sigma_0 + \xi_0)[1 + h\nu_c\Gamma/(m_e c^2)]},$$

$$K = \frac{3\sigma_T\sigma_B R_0^\alpha T_c^4 t_{fs}^{1/2}\zeta_\pm}{8m_p c^2 t_r^{1/2}(h\nu_c/m_e c^2)^2}, \quad \text{and} \quad \beta = 1 - \alpha. \tag{33}$$

The equation for the Compton cooling radius R_{CC} is a transcendental equation which can be solved perturbatively after we transform it into the following logarithmic transcendental equation:

$$\frac{A}{R_{CC}} = \log(K) + \beta\log(R_{CC}). \tag{34}$$

At the zeroth order, $\log(R_{CC})$ term on the right-hand side of the above equation is neglected and, the solution is

$$R_{CC}^* = \frac{A}{\log(K)}, \tag{35}$$

which, when substituted back into (34), provides the first order solution for the Compton cooling radius

$$R_{CC} = \frac{A}{\log(K) + \beta\left[\log(A) - \log(\log(K))\right]}. \tag{36}$$

The estimate for R_{CC} using equation (36) and the exact solution of equation 32 for fixed parameters $L_{50} = 1$, $\theta_j = 0.1$, $T_{0,7} = 1$, $\Gamma_2 = 1$, $\sigma_{0,6} = 1$, $\zeta_\pm = 1$ and $\alpha = 1/2$ are $R_{CC}(\alpha = 1/2) = 7.17 \times 10^9$ cm and $R_{CC}(\alpha = 1/2) = 7.23 \times 10^9$ cm, respectively.

The radius is proportional to L_{52}, inversely proportional to σ_0, and has a very weak dependence on α.

4 SHIELDING JETS FROM IC DRAG BY CREATION OF ELECTRONS AND POSITRONS

Thus far, we have assumed that the jet energy is carried outward by magnetic fields, protons and electron–positron pairs. However, we have not estimated the number of $e^\pm$ that might have been produced in the hot plasma at the base of the jet, or pairs that might be created in the collision of IC-scattered photons. The presence of these pairs could shield the inner part of the jet from IC drag due to thermal photons from the cocoon. In the next sub-section, we take up the calculation of thermal $e^\pm$ that owe their existence to the initial hot plasma at the base of the jet, and show that their number density is too small far away from the jet launching site to be able to shield the jet. In Section 4.2, we provide an estimate of the density of pairs generated when thermal photons from the cocoon collide with photons that are IC scattered by $e^\pm$ in the jet. This process is shown to be effective in shielding the jet for a while but eventually pairs annihilate and pair screen disappears exposing the jet–core to severe IC drag (Section 4.2).

4.1 Thermal pairs and shielding of Poynting jets

The number density of *thermal* pairs at any r is given by the standard thermal distribution formula corresponding to the local temperature of the jet as long as the $e^\pm$ annihilation time is less than the dynamical time.[2] The radius where the two time-scales become equal, $R_{\rm freeze}$, is the freeze-out radius for pairs. Beyond this radius, the total number of $e^\pm$ does not change barring the dissipation of jet kinetic, or magnetic, energy and using that to create new pairs; non-thermal pair creation will be taken up in Section 4.2. We calculate the number density of pairs at $R_{\rm freeze}$ and show that to be much smaller than the density of protons. Therefore, thermal pairs are unimportant for shielding the jet.

The temperature at the base of a Poynting jet is

$$k_{\rm B}T_0 \approx k_{\rm B}\left[\frac{\xi_0 L^{\rm iso}}{4\pi R_0^2 \sigma_{\rm B}(\sigma_0+\xi_0)}\right]^{1/4} \approx (41\,{\rm keV})\,(\xi_0 L_{52}^{\rm iso}/\sigma_{0,6})^{1/4} R_{0,7}^{-1/2}, \tag{37}$$

which is considerably smaller than the temperature for a thermal fireball with $\sigma_0 < 1$; $L^{\rm iso} \equiv 4L/\theta_{\rm j}^2$ is isotropic equivalent of jet luminosity ($\theta_{\rm j} \sim 1$ at the jet base).

Considering the conservation of entropy in a shell of plasma as it moves to larger radius with the jet, we find the decrease of comoving frame temperature with r

$$T'(r) \sim T_0\left(\frac{R_0}{r}\right)^{2\alpha/3}\Gamma^{-1/3} \sim T_0\left(\frac{R_0}{r}\right)^{\alpha}, \tag{38}$$

where we have made use of equation (8) for the transverse size of the jet and equation (7) for Γ; as noted above equation (8), $\alpha \sim 0.5$ in the helium-envelope of GRB progenitor star.

The cross-section for pair annihilation when the average thermal speed of $e^\pm$ is $v_\pm$ is $\sigma_{\rm T}/(v_\pm/c)$. The annihilation time for a positron in jet comoving frame, given the density of electrons to be $n'_\pm/2$, is therefore

$$t'_{\rm ann} \approx \frac{2}{\sigma_{\rm T}n'_\pm c}. \tag{39}$$

The pair annihilation ceases, and their total number freezes, at a radius where $t'_{\rm ann} \sim r/c\Gamma(r)$. Thus, the freeze-out radius is given by

$$R_{\rm freeze} \sim \frac{2\Gamma}{\sigma_{\rm T}n'_\pm}, \tag{40}$$

and the pair density at $R_{\rm freeze}$ is

$$n'_\pm(R_{\rm freeze}) \approx \frac{2\Gamma(R_{\rm freeze})}{\sigma_{\rm T}R_{\rm freeze}}. \tag{41}$$

To determine the pair freeze-out radius, we substitute for thermal pair density, i.e. the following equation

$$n'_\pm = \frac{2(2\pi k_{\rm B}m_{\rm e}T')^{3/2}}{h^3}\exp\left(-m_{\rm e}c^2/k_{\rm B}T'\right), \tag{42}$$

and r dependence of Γ and T' into equation (40):

$$\exp\left\{\frac{5.9\times10^9}{T_0}\left(\frac{R}{R_0}\right)^\alpha\right\} \sim \frac{R_0 T_0^{3/2}}{6.2\times10^8}\left(\frac{R_0}{R}\right)^{5\alpha/2-1}. \tag{43}$$

Let us define

$$C \equiv \frac{5.9\times10^9}{T_0}, \quad {\rm and} \quad D \equiv \frac{R_0 T_0^{3/2}}{6.2\times10^8}, \tag{44}$$

and rewrite equation (43) as

$$C\left(\frac{R}{R_0}\right)^\alpha = \log(D) + \left(\frac{5}{2}\alpha-1\right)\log\left(\frac{R_0}{R}\right), \tag{45}$$

which is easier to solve analytically. Neglecting, at first, the $\log R$-term on the right-hand side, we find $R = ((\log D)/C)^{1/\alpha}$. Substituting that back into equation (45), the approximate analytical solution for the freeze-out radius is found to be

$$\left(\frac{R_{\rm freeze}}{R_0}\right) \sim \frac{1}{C^{1/\alpha}}\left[\log(D)+\left(\frac{5}{2}-\frac{1}{\alpha}\right)(\log(\log(D))-\log(A))\right]^{1/\alpha}. \tag{46}$$

The results for the freeze-out radius obtained as exact numerical solution of equation (43) are in good agreement with the above-approximated expression.

The freeze-out radius has a weak dependence on α, and for $\sigma_0 = 10^6$ and $T_0 = 41$ keV, pair density freezes out fairly close to the jet launching site.

The temperature at freeze-out can be calculated using equation (38), and it can be shown to be $T'_{\rm freeze} \approx 10$ keV that is almost independent of various parameters. The isotropic equivalent luminosity carried by pairs for $r \geq R_{\rm freeze}$ is

$$L_\pm^{\rm iso} \approx 4\pi R_{\rm freeze}^2 m_{\rm e}c^3 n'_\pm\Gamma^2 \approx 4\pi R_{\rm freeze}m_{\rm e}c^3\Gamma^3/\sigma_{\rm T}$$

$$\approx \frac{4\pi R_0 m_{\rm e}c^3}{\sigma_{\rm T}}\left(\frac{R_{\rm freeze}}{R_0}\right)^{1+3\alpha}, \tag{47}$$

where we made use of equation (41) for pair density at $R_{\rm freeze}$, or

$$\frac{L_\pm^{\rm iso}}{L^{\rm iso}} \sim 5\times10^{-16}\frac{R_{0,7}}{L_{52}^{\rm iso}}\left[2L_{52}^{{\rm iso}1/4}R_{0,7}^{-1/2}\sigma_{0,6}^{-1/4}\right]^{(3\alpha+1)/\alpha}. \tag{48}$$

The jet kinetic luminosity at r is $L/\sigma(r)$, and we see from the above equation that thermal pairs are insignificant carriers of jet kinetic luminosity – most of the kinetic luminosity is being carried by protons. The ratio of $e^\pm$ pair to proton number density above the freeze-out radius is given by

$$\frac{n'_\pm}{n'_{\rm p}} \sim 10^{-12}\sigma(R_{\rm freeze})L_{52}^{{\rm iso}-1}R_{0,7}\left[2L_{52}^{{\rm iso}1/4}R_{0,7}^{-1/2}\sigma_{0,6}^{-1/4}\right]^{(3\alpha+1)/\alpha}, \tag{49}$$

---

[2] A more precise statement is that number density of pairs at any given radius is given by the balance between creation and annihilation rates. However, it can be shown that the assumption of thermal equilibrium is approximately valid as long as annihilation time is short compared with the expansion time.

where $\sigma(R_{\rm freeze}) \sim \sigma_0/\Gamma(R_{\rm freeze})$ is the magnetization parameter at $r = R_{\rm freeze}$. Substituting this expression for $\sigma(R_{\rm freeze})$ back into equation (49), it becomes

$$\frac{n'_{\pm}}{n'_{\rm p}} \sim 10^{-6}\sigma_{0,6}\left(\frac{R_0}{R_{\rm freeze}}\right)^{\alpha} L_{52}^{\rm iso-1} R_{0,7}$$

$$\times \left[2L_{52}^{\rm iso1/4}R_{0,7}^{-1/2}\sigma_{0,6}^{-1/4}\right]^{(3\alpha+1)/\alpha}. \tag{50}$$

Equation (50) shows that thermal pairs are too small in number to affect the propagation of photons into the jet, and hence they cannot shield the jet from the severe IC drag.

4.2 Pair creation due to photon collisions and shielding of jet from IC drag

The calculation in previous sections ignored the possibility that thermal photons IC scattered by the jet might have sufficient energy for electron–positron pair creation. These IC-scattered photons could give rise to an optically thick layer of $e^{\pm}$ on the side wall of the jet that is in contact with the cocoon, and this could potentially shield the interior of the jet from IC drag. We investigate that possibility in this sub-section.

Let us consider the mean frequency of thermal photons in the cocoon to be $\nu_{\rm c}$, and after colliding with an electron in the jet with Lorentz factor Γ the frequency increases to $\nu_{\rm ic}$ (these frequencies are in the rest frame of the star). The scattered photon travels within an angle Γ^{-1} of the electron's velocity vector due to relativistic beaming, and hence its chances of undergoing a second collision with another electron is drastically reduced since the photon is moving in nearly the same direction as electrons in the jet.

The condition for pair production when averaged over the angle between colliding photons is: $(h\nu_{\rm ic})(h\nu_{\rm c}) > 2m_{\rm e}^2 c^4$ (e.g. Gould & Schréder 1967). Since $h\nu_{\rm ic} \sim m_{\rm e}c^2\Gamma/2$ (equation 24) for large angle collisions in the Klein–Nishina regime – i.e. when $h\nu_{\rm c}\Gamma > m_{\rm e}c^2$ – the pair production condition becomes $h\nu_{\rm c}\Gamma \gtrsim 4m_{\rm e}c^2$. Thus, for a given cocoon temperature ($T_{\rm c}$) at a certain radius where jet Lorentz factor becomes larger than the following critical value:

$$\Gamma_{\rm crit} \sim \frac{4m_{\rm e}c^2}{3k_{\rm B}T_{\rm c}}, \tag{51}$$

pair production at the interface of the jet and cocoon begins. For cocoon temperature of $\sim$10 keV, $\Gamma_{\rm crit} \sim 70$. The Lorentz factor of magnetic jets increases with radius as $\sim r^{1/2}$, and therefore $\Gamma \sim 10^2$ can be attained near the stellar surface where the jet also becomes transparent in the transverse direction (in the absence of $e^{\pm}$) for $\sigma_0 > 10^6$; the Lorentz factor of a thermally driven jet increases more rapidly with r, and it too is likely to develop an $e^{\pm}$ layer surrounding it before reaching the stellar surface.

For the remainder of this section, we assume that the condition for pair production is satisfied, and describe the effect that has on jet structure and dynamics.

The distance travelled by a high energy IC photon – which is moving almost parallel to the jet axis (within an angle Γ^{-1} to be precise) – before it is turned into $e^{\pm}$ as a result of collision with a thermal photon from the cocoon is

$$\lambda_{\gamma} = (\sigma_{\pm}n_{\gamma})^{-1} \sim (2 \times 10^2 \,\text{cm})\, t^{1/2} R_{*,11}^{1/2}(L_{50}/\theta_{j,-1})^{-1/4}\eta_{\rm c,1}^{-3/8}, \tag{52}$$

where $\sigma_{\pm}$ is the cross-section for $\gamma + \gamma \rightarrow e^- + e^+$ (the maximum value for $\sigma_{\pm}$ is 2.5×10^{-25} cm^2 at photon energy 1.4 times the

threshold value given above (e.g. Svensson 1982),

$$n_{\gamma}(t) \sim \frac{F_{\rm c}(t)}{h\nu_{\rm c}c} \sim (1.8 \times 10^{22} \,\text{cm}^{-3})\, t^{-1/2} R_{*,11}^{-1/2}(L_{50}/\theta_{j,-1})^{1/4}\eta_{\rm c,1}^{3/8}, \tag{53}$$

is the number density of thermal photons at the interface of the co-coon and the jet at time t (in seconds) in star rest frame, $\nu_{\rm c} = 3k_{\rm B}T_{\rm c}$ and $F_{\rm c}(t)$ are given by equations (A16) and (A23). We see from equation (52) that high-energy IC photons do not travel very far from their place of creation before undergoing pair production. The newly produced $e^{\pm}$s have thermal Lorentz factor less than $\sim$2 in jet comoving frame[3] but they cool rapidly via the synchrotron process on a time-scale much smaller than the dynamical time; magnetic field in the jet comoving frame is $B' = (4L/\theta_{\rm j}^2\Gamma^2 r^2 c)^{1/2} = (1.2 \times 10^8 \,\text{G})L_{50}^{1/2}/[\theta_{\rm j,-1}\Gamma_2 r_{11}]$, and hence the synchrotron cooling time in jet comoving frame is $\sim$(5×10^{-8} s) $[\theta_{\rm j,-1}\Gamma_2 r_{11}]^2 L_{50}^{-1}$.

The rate of pair production per electron is approximately equal to the number of photons it scatters per unit time, i.e.

$$\frac{\dot{n}_{\pm}}{n_{\rm e}} \approx \frac{\sigma_{\rm T}n_{\gamma}c}{1 + h\nu_{\rm c}\Gamma/(m_{\rm e}c^2)} \approx (3 \times 10^7 \,\text{s}^{-1})t^{-1/2}\Gamma_2^{-1}\eta_{\rm c,1}^{1/2}. \tag{54}$$

The second equality is obtained for the case where thermal photons from the cocoon are scattered by electrons in the jet in Klein–Nishina regime, i.e. $h\nu_{\rm c}\Gamma/(m_{\rm e}c^2) = 3k_{\rm B}T_{\rm c}\Gamma/(m_{\rm e}c^2) \gg 1$, and in that case we find the surprising result that the rate of pair production per electron depends only on the Lorentz factors of the jet and cocoon.[4] Once pair production starts, it proceeds rapidly since newly produced $e^{\pm}$ also IC scatter thermal photons which have sufficient energy for more pair production. However, the number of pairs produced per proton cannot much exceed $m_{\rm p}\Gamma/(m_{\rm e}\Gamma_{\rm crit})$ because the Lorentz factor of protons and $e^{\pm}$ in that case drops below $\Gamma_{\rm crit}$ (in order to conserve momentum), and IC scattered photons then no longer have sufficient energy for further production of pairs. Thus, pair production saturates on a time-scale

$$t_{\rm sat} \sim (3 \times 10^{-8} \,\text{s})t^{1/2}\,\Gamma_2\,\eta_{\rm c,1}^{-1/2}\ln\left[m_{\rm p}\Gamma/m_{\rm e}\Gamma_{\rm crit}\right]. \tag{55}$$

The physical thickness of the pair screen corresponding to optical depth unity, $\Delta_{\pm}(\tau_{\pm} = 1)$, is given by

$$\Delta_{\pm}(\tau_{\pm} = 1) = \frac{(m_{\rm e}/m_{\rm p})}{\sigma_{\rm T}n_{\rm p}(\Gamma/\Gamma_{\rm crit})}$$

$$\sim (1.2 \times 10^5 \,\text{cm})\frac{R_{*,11}^2(\sigma_{0,6} + \xi_{0,6}\theta_{j,-1}^2)}{L_{50}}, \tag{56}$$

where $n_{\rm p}$ is proton density in the jet at $r = R_*$ which is given by equation (17), and ξ_0 is thermal energy per proton divided by $m_{\rm p}c^2$ at the base of the jet.

We note that as long as the Lorentz factor of $e^{\pm}$ is larger than $\Gamma_{\rm crit}$, gamma-rays from pair annihilation are converted back to $e^{\pm}$ within a short distance of a few metres (equation 52) due to collisions with thermal photons from the cocoon. Pair production process is terminated when the Lorentz factor of the screen falls below $\Gamma_{\rm crit}$ and its optical depth becomes so large that X-ray photons from the cocoon are prevented from entering the faster moving interior of the jet where $\Gamma > \Gamma_{\rm crit}$.

Let us consider that the optical depth of $e^{\pm}$ layer surrounding the jet at radius r is $\tau_{\pm}(r)$. The flux of photons from the cocoon that

---

[3] Newly produced pairs are swept up by the magnetic field in the jet and forced to move with the outflow.

[4] The time dependence for pair production rate of $t^{-1/2}$ (equation 54) is due entirely to the cocoon thermal flux $F_{\rm c}$.
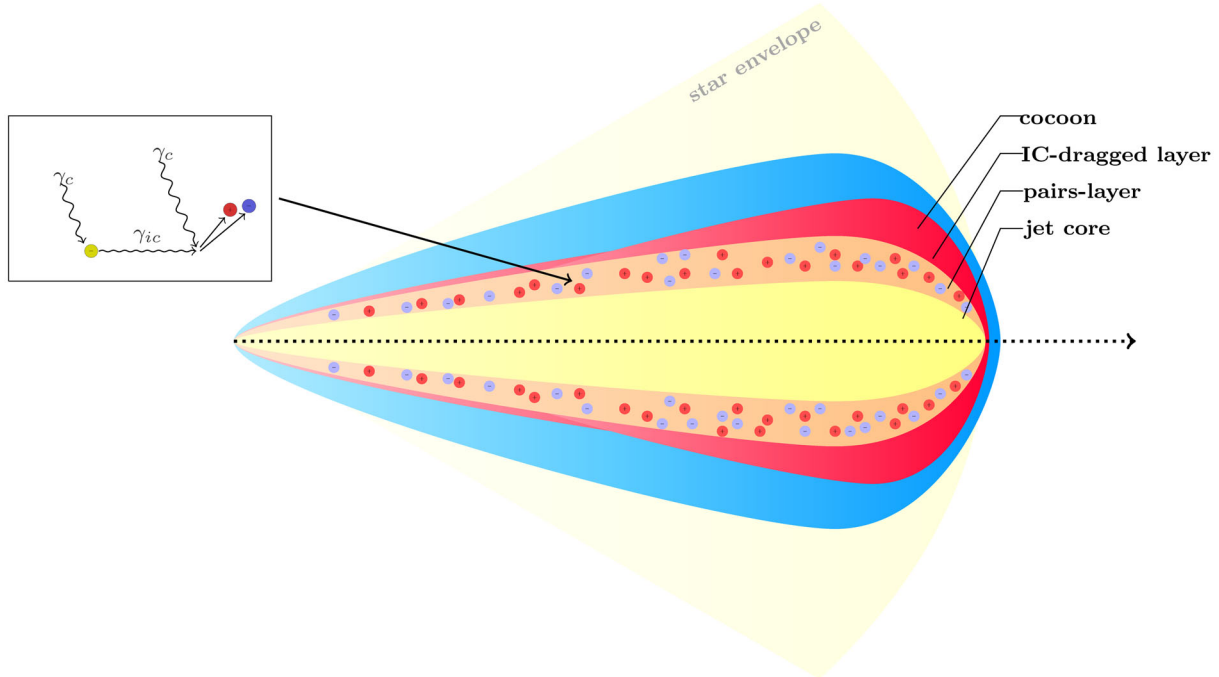
Figure 2. Schematic view of the layered jet structure while it has been braked by the IC interaction with the hot photons from the cocoon. If the magnetization parameter σ is larger than 10^7, the jet build up a self-shielding e^+/e^--pair screen created by photons from the cocoon and IC-scattered photons.

crosses this layer is

$$f_{n_\gamma}(t, \tau_\pm) \approx \frac{F_c(t)\exp(-\tau_\pm)}{3k_B T_c} \sim (5.5 \times 10^{38}\,\mathrm{cm}^{-2}\,\mathrm{s}^{-1})$$
$$\times \exp(-\tau_\pm)\frac{L_{50}^{1/4}\eta_{c,1}^{3/8}}{\theta_{j,-1}^{1/4} R_{*,11}^{1/2} t^{1/2}}, \qquad (57)$$

where we made use of equations (A16) and (A23). Pair production can proceed in the interior to the $e^\pm$ screen as long as the distance travelled by an IC-scattered photon before it collides with a thermal photon (equation 52) is smaller than R_*, i.e.

$$\lambda_\gamma \sim (2 \times 10^2\,\mathrm{cm})\,e^{\tau_\pm}\,t^{1/2}\,R_{*,11}^{1/2}\,(L_{50}/\theta_{j,-1})^{-1/4}\eta_{c,1}^{-3/8} < R_*. \quad (58)$$

Moreover, the time it takes for a photon from the cocoon to cross this layer should also be less than R_*/c. Thus, we find that the optical depth of the screen is

$$\tau_\pm \sim 20 + \log\left[t^{-1/2}\,R_{*,11}^{-1/2}(L_{50}/\theta_{j,-1})^{1/4}\eta_{c,1}^{3/8}\right], \qquad (59)$$

and the physical thickness of the pair screen is max $\{20\Delta_\pm, R_*/\Gamma\}$, where $\Delta_\pm$ is given by equation (56); pair screen thickness is R_*/Γ when IC photons – moving at an angle Γ^{-1} with respect to the jet axis – travel a distance R_* before colliding with thermal photons from the cocoon.

Electrons and positrons in the pair screen continue to scatter X-ray photons from the cocoon and the resulting drag slows down the jet below Γ_{crit} (Fig. 2). The time it takes for Γ to fall below Γ_{crit} is of the order of 10^{-4} s $\exp(\tau_\perp)/\zeta_\pm$ (equation 28). When the Lorentz factor of pairs falls below Γ_{crit} (equation 51), gamma-rays produced in pair annihilation no longer have sufficient energy for pair creation, and at that time the pair screen begins to evaporate.

The time (measured in the rest frame of the star) for a positron to run into an electron and annihilate is

$$t_{e^\pm,an}(r) = \frac{\Gamma^2}{\sigma_{e^\pm->\gamma\gamma}n_\pm v_\pm} = \frac{\Gamma^2}{\sigma_T n_\pm c}$$
$$\sim (5 \times 10^2\,\mathrm{s})\frac{\Gamma_2^2 r_{11}^2(\sigma_{0,6} + \xi_{0,6})}{\zeta_\pm L_{52}^{iso}}, \qquad (60)$$

where $\sigma_{e^\pm->\gamma\gamma} = \sigma_T/(v_\pm/c)$ is annihilation cross-section, $v_\pm$ is the average relative speed between electrons and positrons in jet comoving frame and $n_\pm \sim \zeta_\pm n_p$ is the pair density; for $\zeta_\pm \sim (m_p/2m_e)(\Gamma/\Gamma_{crit})$, i.e. the maximum possible number of pairs per protons when $\Gamma > \Gamma_{crit}$, the annihilation time is ~ 0.3 s. The ratio of annihilation and dynamical times at radius r is

$$\frac{t_{e^\pm,an}(r)}{t_{dyn}} \sim 1.5 \times 10^2 \frac{\Gamma_2^2 r_{11}(\sigma_{0,6} + \xi_{0,6})}{\zeta_\pm L_{52}^{iso}}, \qquad (61)$$

which is smaller than 1 for $r \lesssim 10^9$ cm even for $\zeta_\pm = 1$, and that means that any pairs produced at the base of the jet or at any radius smaller than 10^9 cm cannot survive as the jet moves to larger radii. Hence, only an ongoing process of pair formation can support $\zeta_\pm > 1$.

The Lorentz factor of pair screen continues to decrease due to IC drag and that causes the annihilation time – which scales as Γ^2 (equation 60)[5] – to decrease rapidly. Since the time-scale for the

---

[5] For a time-independent relativisic outflow, particle density in star rest frame does not vary as we follow the flow-streamlines even though the Lorentz factor might increase or decrease. This is due to the conservation of particle flux and the fact that the speed is a constant c for a relativistic system. The particle density along a flow-line, of course, varies as Γ^{-1} in the comoving frame of the outflow.

creation of pair screen is smaller than the IC drag time which is much smaller than the pair annihilation time, soon after the pair screen forms its Lorentz factor decreases rapidly to order unity (on 0.1 μs time – equation 29), pairs annihilate and screen evaporates on time-scale of the order of 1 ms (equation 60). Once the optical depth of the screen decreases, photons from the cocoon pass through it, and the process of formation of $e^{\pm}$ and IC drag progresses deeper inside the jet. At any given radius, this process is only terminated at a distance from jet axis where the Thompson optical depth out to the jet–cocoon boundary, for $\zeta_{\pm} \sim 1$, is of the order of 10. Hence, as we get closer to the stellar surface, we find an increasingly larger fraction of the jet to have gone through the process of forming pair screen, $e^{\pm}$ annihilation and IC drag. If the jet with $\zeta_{\pm} = 1$ becomes transparent in the transverse direction near the stellar surface – as it in fact does for $\sigma_0 \gtrsim 10^6$ according to equation (13) – then self-generated pair screen is too short lived to protect it from IC drag. It should be noted that that the transient nature of the pair screen in fact speeds up the process of jet IC drag because the drag time is proportional to $\zeta_{\pm}^{-1}$ (see equations 28–29).

Although very high-σ jets ($\sigma_0 \gtrsim 10^6$) are unlikely to survive their passage through the GRB progenitor star and cocoon, they do not disappear without leaving an observational signature. Annihilation of pairs in the screen when the jet Lorentz factor decreases from $\Gamma_{\rm crit}$ to of order unity produces photons of energy between 0.5 MeV and $\sim m_e c^2 \Gamma_{\rm crit} \sim 50$ MeV which can escape the jet in the longitudinal direction to arrive at the observer. The jet is slowed down by pair creation and IC drag, and these processes are about equally important for decelerating the jet. Hence, the observer-frame luminosity carried by pairs is of the order of the jet kinetic luminosity or L_j/σ (where σ is the magnetization parameter of the jet when it is near the stellar surface). The total energy carried by the photons resulting from pair annihilation is of the order of the energy of the pairs, and therefore, the total luminosity of pair annihilation photons, L_γ, is of the order of L/σ. The duration of the annihilation pulse we expect to be of the order of the activity time of the central engine, which for long GRBs is typically around 5–100 s.

The picture that emerges is that the outer layers of GRB jets are slowed down due to IC drag. However, inner regions continue to accelerate with r, and at some radius their Lorentz factor exceeds $\Gamma_{\rm crit}$. At that point, a very rapid generation of $e^{\pm}$ ensues provided that the optical depth of the slower moving layer outside of this region is less than about 20. The IC drag slows down the pair screen rather quickly and then $e^{\pm}$ annihilate on a relatively short time-scale of ~ 1 ms, and the formation of a new pair screen moves closer to the jet axis. This process continues until the jet becomes opaque in the transverse direction due to just the electrons associated with protons, i.e. for $\zeta_{\pm} = 1$. Jets of initial magnetization (σ_0) smaller than 10^6 are sufficiently opaque in transverse direction even when they rise above cocoon surface that they are essentially protected from IC drag. However, photons from the cocoon can penetrate a jet all the way to its axis when $\sigma_0 \gtrsim 10^6$, and the strong IC drag then slows down the outflow to sub-relativistic speed. It turns out that high-σ jets cannot escape this fate in spite of the $e^{\pm}$ pair screen they create because these screens are rather short lived.

5 CONCLUSIONS

Relativistic jets in GRBs are surrounded by a hot cocoon of plasma that was created during the initial passage of the jet through the star when it shock heated the gas along its path and pushed it sideways to clear a cavity through the polar region of the GRB progenitor star. Thermal photons from this cocoon are scattered by electrons in

the jet and that provides a strong drag force on the jet. Jets of initial magnetization parameter (σ_0) smaller than about 10^6 are highly opaque in the transverse direction while travelling inside the GRB progenitor star, and thus they have a core region that is protected from this IC drag. The outer layers of this jet (about 20 Thompson optical depth thick), however, suffer IC drag and are slowed down considerably.

Jets with $\sigma_0 \gtrsim 10^6$ are transparent to photons from the cocoon near the stellar surface, and they are slowed down to sub-relativistic speeds due to IC drag. This is in spite of the fact that an optically thick layer of electrons and positrons forms at the interface of the cocoon and jet and that tries to protect the core of the jet from IC drag (Fig. 2); these pairs are formed by the collisions of thermal photons from the cocoon with high-energy photons that are produced when cocoon photons are IC scattered by the jet. However, the problem is that the pair screen itself slows down rapidly due to IC drag, and that causes pairs to annihilate and the $e^{\pm}$-shield to evaporate rather quickly. Pair production then moves closer towards the jet axis, and the story is repeated until the entire jet is slowed down by the IC drag.

The process of pair screen formation and annihilation associated with a high-σ jet has observational consequences. For jets with $\sigma_0 \gtrsim 10^6$, we should see a pulse of high-energy photons of energy between ~ 1 MeV and $\sim m_e c^2 \Gamma_{\rm crit} \sim 50$ MeV with luminosity of the order of the Poynting jet luminosity. The duration of this pulse should be of the order of the central engine activity time.

Even Poynting jets of $\sigma_0 \lesssim 10^6$ – which are highly opaque in the transverse direction – might suffer effects of IC drag indirectly. As the outer layers of these jets are slowed down by IC scatterings, the resulting shear instabilities might slow down the inner regions as well. Moreover, if magnetic field lines thread the outer and the inner regions of the jet, then slowing down of the outer part of the jet would get communicated to the inner region, and that could affect the entire jet. The details of this would depend on the magnetic field configuration and that is something that needs to be looked into.

If a highly magnetized jet manages to escape IC drag while travelling inside the GRB progenitor star – for instance, if it is encapsulated inside a highly opaque baryonic outflow to shield it from X-rays from the cocoon – it would be subjected to rapid dissipation due to charge starvation before reaching the deceleration radius (Appendix B).

ACKNOWLEDGEMENTS

REFERENCES

Berger E., Kulkarni S. R., Frail D. A., 2003, ApJ, 590, 379
Blandford R. D., Znajek R. L., 1977, MNRAS, 179, 433
Blumenthal G. R., Gould R. J., 1970, Rev. Mod. Phys., 42, 237
Bromberg O., Granot J., Lyubarsky Y., Piran T., 2014, MNRAS, 443, 1532
Bromberg O., Nakar E., Piran T., Sari R., 2011, ApJ, 740, 100
Bucciantini N., Quataert E., Arons J., Metzger B. D., Thompson T. A., 2008, MNRAS, 383, L25
Bucciantini N., Quataert E., Metzger B. D., Thompson T. A., Arons J., Del Zanna L., 2009, MNRAS, 396, 2038
Cenko S. B. et al., 2010, ApJ, 711, 641
Curran P. A., van der Horst A. J., Wijers R. A. M. J., 2008, MNRAS, 386, 859
Falcke H., Körding E., Markoff S., 2004, A&A, 414, 895
Frail D. A. et al., 2001, ApJ, 562, L55

Gehrels N., Ramirez-Ruiz E., Fox D. B., 2009, ARA&A, 47, 567
Ghisellini G., Tavecchio F., 2010, MNRAS, 409, L79
Ghisellini G., Tavecchio F., Chiaberge M., 2005, A&A, 432, 401
Gould R. J., Schréder G. P., 1967, Phys. Rev., 155, 1408
Kumar P., Zhang B., 2014, preprint (arXiv:1410.0679)
Lazzati D., Begelman M. C., 2005, ApJ, 629, 903
Liang E.-W., Racusin J. L., Zhang B., Zhang B.-B., Burrows D. N., 2008, ApJ, 675, 528
Markoff S., 2010, in Belloni T., ed., Lecture Notes in Physics, Vol. 794, The Jet Paradigm. Springer-Verlag, Berlin, p. 143
Markoff S., Nowak M. A., Wilms J., 2005, ApJ, 635, 1203
Matzner C. D., 2003, MNRAS, 345, 575
Melia F., Konigl A., 1989, ApJ, 340, 162
Meszaros P., 2006, Rep. Prog. Phys., 69, 2259
Metzger B. D., Giannios D., Thompson T. A., Bucciantini N., Quataert E., 2011, MNRAS, 413, 2031
Metzger B. D., Thompson T. A., Quataert E., 2007, ApJ, 659, 561
Mizuta A., Aloy M. A., 2009, ApJ, 699, 1261
Mizuta A., Ioka K., 2013, ApJ, 777, 162
Morsony B. J., Lazzati D., Begelman M. C., 2007, ApJ, 665, 569
Narayan R., McClintock J. E., 2008, New Astron. Rev., 51, 733
O'Brien P. T. et al., 2006, ApJ, 647, 1213
Panaitescu A., Kumar P., 2001, ApJ, 560, L49
Phinney E., 1987, in Zensus J. A., Pearson T. J., eds, Superluminal Radio Sources. Cambridge Univ. Press, Cambridge, p. 301
Piran T., 1999, Phys. Rep., 314, 575
Racusin J. L. et al., 2009, ApJ, 698, 43
Ramirez-Ruiz E., Celotti A., Rees M. J., 2002, MNRAS, 337, 1349
Sari R., Piran T., Halpern J. P., 1999, ApJ, 519, L17
Sikora M., Sol H., Begelman M. C., Madejski G. M., 1996, MNRAS, 280, 781
Svensson R., 1982, ApJ, 258, 335
Tagliaferri G. et al., 2005, Nature, 436, 985
Thompson T. A., Chang P., Quataert E., 2004, ApJ, 611, 380
Willingale R., Genet F., Granot J., O'Brien P. T., 2010, MNRAS, 403, 1296
Woosley S. E., Bloom J. S., 2006, ARA&A, 44, 507
Yuan F., Narayan R., 2014, ARA&A, 52, 529

APPENDIX A: RADIATION FROM COCOON SURROUNDING RELATIVISTIC JET

We describe in this appendix a simplified, analytical, treatment of cocoon dynamics and radiation. This follows the work of Ramirez-Ruiz, Celotti & Rees (2002) and Matzner (2003) except for one thing and that is that we do not assume that the jet is conical in shape while inside the star. Numerous investigations of relativistic jets, e.g. Lazzati & Begelman (2005), Morsony, Lazzati & Begelman (2007), Mizuta & Aloy (2009), Mizuta & Ioka (2013), Bromberg et al. (2011, 2014) have shown that the cocoon created by the jet can be very effective in collimating it, and hence we take the jet opening angle to be a function of distance from the centre.

The energy in the cocoon (E_c) is of the order of the energy carried by the jet while it makes its way through the polar region of the GRB progenitor star, i.e.

$$E_c \sim L R_* / v_h, \tag{A1}$$

where v_h is the average speed at which the jet head moves through the star. The jet head speed can be calculated from the conservation of momentum flux in the radial direction of the unshocked stellar gas as viewed from the rest frame of the jet head:

$$\rho_j c^2 (\Gamma_j^2 / 4\Gamma_h^2) \approx \rho_a \Gamma_h^2 v_h^2, \tag{A2}$$

where ρ_j and ρ_a are densities of the unshocked jet and the stellar envelope, respectively, and Γ_j and Γ_h are the Lorentz factors of the unshocked jet and the jet head with respect to the unshocked star

(the Lorentz factor of the unshocked jet with respect to jet head is $\Gamma_j / 2\Gamma_h$). Considering that the jet luminosity at the stellar surface can be written as

$$L = \pi \theta_j^2 R_*^2 \rho_j \Gamma_j^2 c^3, \tag{A3}$$

and the mass of the swept-up gas by the jet is

$$m_c \sim \pi \theta_j^2 \rho_a R_*^3, \tag{A4}$$

we obtain

$$2\Gamma_h^2 v_h \sim \left[\frac{R_* L}{c m_c} \right]^{1/2}, \tag{A5}$$

where θ_j is jet opening angle which is a function of distance from the centre due to collimation provided by the cocoon. We can simplify this expression further by substituting for L using equation (A1)

$$4\Gamma_h^4 v_h \sim c \eta_c \tag{A6}$$

where

$$\eta_c \equiv \frac{E_c}{m_c c^2} \tag{A7}$$

is the terminal Lorentz factor of the cocoon plasma (provided that $\eta_c \geq 1$) after it escapes through the stellar surface and its thermal energy is converted to bulk kinetic energy.

Therefore, the jet head speed is sub-relativistic when $\eta_c < 4$ and is given by

$$v_h \sim c \eta_c / 4. \tag{A8}$$

For $\eta_c > 4$, the jet head speed is relativistic and its Lorentz factor is given by

$$\Gamma_h \sim (\eta_c / 4)^{1/4}. \tag{A9}$$

The expansion speed of the cocoon in the direction perpendicular to its surface, v_c, is determined by equating the ram pressure with the thermal pressure inside the cocoon (p_c), e.g. Matzner (2003),

$$v_c = (p_c / \rho_a)^{1/2}. \tag{A10}$$

The average thermal pressure inside the cocoon is approximately

$$p_c \sim \frac{E_c}{3 V_c}. \tag{A11}$$

where

$$V_c \sim \pi t^3 v_h v_c^2 / 3 \sim R_*^3 (v_c / v_h)^2 \tag{A12}$$

is the volume of the cocoon at the time it emerges at the stellar surface. Combining equations (A10) and (A11), we find

$$v_c^4 \sim \frac{E_c v_h^2}{3 \rho_a R_*^3} \sim \theta_j^2 \eta_c v_h^2 c^2 / 3. \tag{A13}$$

Substituting for v_h from equations (A8) and (A9), we find

$$\frac{v_c}{c} \sim \begin{cases} (\theta_j^2 \eta_c^3 / 48)^{1/4} & \text{for } \eta_c < 4 \\ (\theta_j^2 \eta_c / 3)^{1/4} & \text{for } 4 < \eta_c < \theta_j^{-2}. \end{cases} \tag{A14}$$

The thermal pressure of the cocoon can be obtained using equations (A10) and (A14) and is given by

$$p_c \sim \frac{L}{\theta_j R_*^2 c (3\eta_c)^{1/2}}, \tag{A15}$$

and its temperature is

$$k_B T_c = k_B (3 p_c / \sigma_a)^{1/4} \sim (24 \text{ keV}) \frac{L_{50}^{1/4}}{\theta_{j,-1}^{1/4} R_{*,11}^{1/2} \eta_{c,1}^{1/8}}, \tag{A16}$$

where σ_a is the radiation constant. We note that the cocoon temperature has a weak dependence on jet luminosity and angular size, and so it is unlikely to be larger than $\sim$30 keV.

The number density of thermal $e^\pm$ pairs at temperature T_c is given by

$$n_\pm = \frac{2(2\pi k_B m_e T_c)^{3/2}}{h^3} \exp\left(-m_e c^2/k_B T_c\right). \tag{A17}$$

Therefore, for $k_B T_c = 20$ keV, $n_\pm = 1.1 \times 10^{17}$ cm^{-3}, and for 30 keV cocoon temperature $n_\pm = 1.1 \times 10^{21}$ cm^{-3}. We next calculate the number of electrons associated with protons in the cocoon, and show that these exceed $e^\pm$ as long as $k_B T < 30$ keV.

The average number density of electrons associated with baryons in the cocoon is

$$n_{e,c} \sim \frac{m_c}{m_p V_c} \sim \frac{3 p_c}{m_p c^2 \eta_c} \sim (1.5 \times 10^{21}\,\text{cm}^{-3}) \frac{L_{50}}{\theta_{j,-1}^2 R_{*,11}^2 \eta_{c,1}^{3/2}}. \tag{A18}$$

The electron number density near the stellar surface, however, is smaller than the average density given above. The density at the stellar photosphere is $\sim 1/(\sigma_T H_\rho)$, where

$$H_\rho = C_s^2/g \sim (10^8\,\text{cm}) T_{*,5}^2 R_{*,11}^2 M_{*,1}^{-1}, \tag{A19}$$

is the density scaleheight, C_s is sound speed, T_* is photospheric temperature and $M_{*,1}$ is stellar mass in units of $10\,M_\odot$. Thus, the electron density at the photosphere is of the order of 1.5×10^{16} cm^{-3}, and it increases with depth as $(z/z_*)^{1/(\gamma-1)}$; where $\gamma \sim 1.5$ is the effective polytropic index that describes stratification near the stellar surface, and

$$z_* = H_\rho/(\gamma - 1). \tag{A20}$$

Therefore, pair density in cocoon is larger than proton density at the photosphere as long as $k_B T > 15$ keV, but at a depth of more than a few scaleheight below the photosphere the proton density exceeds $n_\pm$. So the electron density in the cocoon as a function of radius can be written as

$$n_{e,c} \sim n_\pm + \min \left\{ \left(\frac{1}{\sigma_T H_\rho}\right) \left[1 + \frac{(R_* - r)}{z_*}\right]^{1/(\gamma-1)}, \right.$$
$$\left. (1.5 \times 10^{21}\,\text{cm}^{-3}) \frac{L_{50}}{\theta_{j,-1}^2 R_{*,11}^2 \eta_{c,1}^{3/2}} \right\}. \tag{A21}$$

The time in between scattering for a photon (photon mean free time) in the cocoon is given by

$$t_{fs} \sim \frac{1}{\sigma_T c\, n_{e,c}}. \tag{A22}$$

The thermal flux at the interface of the cocoon and the jet is dictated by diffusion of photons in cocoon, and is given by

$$F_c(t) = \sigma_B T_c^4 [t_{fs}/(t + t_{fs})]^{1/2}. \tag{A23}$$

This expression is valid as long as t is less than the cocoon expansion time $\sim R_*/v_h$. The flux at an optical depth τ inside the jet is $f_c(t) \exp(-\tau)$.

APPENDIX B: CHARGE STARVATION OF A POYNTING JET

Let us consider a Poynting jet of isotropic equivalent luminosity L^{iso} and magnetization parameter at its base of σ_0. The magnetic field in the jet is assumed to change direction on a length-scale of ℓ_B (in star rest frame) which corresponds to $\ell'_B = \ell_B \Gamma$ in the jet comoving frame. The current required for supporting this non-zero curl is

$$j' \sim B'c/(4\pi \ell'_B), \tag{B1}$$

where

$$B' = \frac{1}{\Gamma} \left[\frac{L^{iso}}{cr^2}\right]^{1/2} \tag{B2}$$

is magnetic field in jet comoving frame.

The electron density in jet comoving frame for a Poynting jet of high magnetization parameter is obtained using equation (6) and is given by

$$n'_e(r) \approx \frac{\zeta_\pm L^{iso}}{4\pi r^2 m_p c^3 \sigma_0 \Gamma}, \tag{B3}$$

where $\zeta_\pm$ is the number of $e^\pm$ per proton which we know from the discussion in Section 4 should be of the order of unity for $r \gg R_*$.

The current required to support the jet magnetic field must be smaller than the maximum current that can be carried by charged particles in the jet, i.e. $j' < q\, n'_e c$. It follows from this requirement that beyond a certain radius, R_{cs}, the jet becomes charge starved, i.e. it does not have sufficient number of electrons to carry the required current. Using the above equations, we find this radius to be

$$R_{cs} \sim \frac{q \ell_B \Gamma \sqrt{L^{iso}}}{m_p \sigma_0 c^{5/2}} \sim (1.5 \times 10^{17}\,\text{cm}) \sqrt{L_{52}^{iso}} \frac{\ell_{B,7} \Gamma_2}{\sigma_{0,6}}. \tag{B4}$$

This should be compared with the deceleration radius, R_d, where the energy of the medium swept-up and shock heated by the jet is approximately half the total energy of the explosion:

$$R_d \sim \left(\frac{3E^{iso}}{4\pi m_p c^2 n_0 \Gamma^2}\right)^{1/3} \sim (1.2 \times 10^{17}\,\text{cm}) \left[\frac{E_{53}^{iso}}{n_0 \Gamma_2^2}\right]^{1/3}, \tag{B5}$$

where E^{iso} is the isotropic equivalent of total energy carried by the jet, and n_0 is the mean number density of protons in the circumstellar medium of the GRB. Thus, a high magnetization jet that stops accelerating when it attains a Lorentz factor of $\sim \sigma_0^{1/3}$ will become charge starved near the deceleration radius and its magnetic field will dissipate rapidly.

We note that if the jet were to start spreading in the radial direction at $r < R_{cs}$, then it would never become charge starved since in that case the required current (j') and the charge density (n'_e) both decline with radius as r^{-2}.

This paper has been typeset from a TeX/LaTeX file prepared by the author.